



Effects of H_2S and phenanthrene on the activity of Ni and Rh-based catalysts for the reforming of a simulated biomass-derived producer gas



D. Laprune^a, D. Farrusseng^a, Y. Schuurman^a, F.C. Meunier^{a,*}, J.A.Z. Pieterse^b, A.M. Steele^c, S. Thorpe^c

^a Univ Lyon, Université Claude Bernard Lyon1, CNRS, Institut de Recherches sur la Catalyse et l'Environnement de Lyon, IRCELYON, 2, Av. Albert Einstein, F-69626 Villeurbanne, France

^b ECN, Sustainable Proc. Technol., PO 1, NL-1755 ZG Petten, The Netherlands

^c Johnson Matthey Technology Centre (JMTC), Blount's Court, Sonning Common, Reading RG4 9NH, UK

ARTICLE INFO

Keywords:

Methane steam reforming
Nickel
Rhodium
Tar
 H_2S

ABSTRACT

A series of Rh and Ni-based catalysts were tested for the reforming of methane and phenanthrene using a feed composition similar in terms of main components to that of the producer gas obtained from wood gasification. The objective was to identify formulations that would enable reforming methane and tars without the need to purify the producer gas. Phenanthrene was chosen as a representative tar because this compound is produced in significant concentrations during low-temperature gasification of woody biomasses and its three-ring structure favors coke formation. The concentration of H_2S used was set at the higher range of typical values, i.e. 200 ppm, to make these tests more challenging. At 900 °C, 200 ppm of H_2S induced a significantly higher activity loss for methane reforming than that induced by 200 ppm of phenanthrene. The rate of methane consumption in the presence of both poisons varied linearly with the Rh metal surface area. The slight deviation observed at higher loading was in part due to heat and mass transport limitations. The rate of methane consumption per unit of metal surface area was about 5-fold higher on Rh than that on Ni. No information could be derived from the measure of apparent activation energies, due to changes in adsorption coverages of reactants and poisons with temperature. Incomplete conversion of polycyclic aromatic hydrocarbons, well-known coke precursors, was obtained at 875 °C and 850 °C.

1. Introduction

Syngas, a mixture of CO and H_2 , can be obtained from the steam and dry reforming of fossil fuels [1–9] and the gasification of biomasses or carbon-containing wastes [10,11]. The gas (often referred to as “producer gas”) obtained from biomass gasification contains significant concentrations of light hydrocarbons, including methane, and tars that should be reformed to increase syngas yield [12,13]. Tars, a mixture of condensable organic compounds such as mono- and polycyclic aromatic hydrocarbons, are well known coke precursors that can induce a strong deactivation of reforming catalysts and bed blockage.

Ni-based catalysts were shown to convert typical compounds obtained from biomass gasification into low volatility products through condensation reactions and oligomerisation leading to catalyst permanent deactivation in the presence of sulfur at low temperatures, i.e. 600 °C [14]. In contrast, the reforming activity was partly recovered following exposure to sulfur if the temperature was set at 700 °C. Di Carlo et al. reported no deactivation at 800 °C of $\text{Ni}/\text{Ca}_{12}\text{Al}_{24}\text{O}_{33}$ used

for the steam reforming of tars derived from hazelnut shells gasification [15]. Sato and Fujimoto observed stable naphthalene conversions at 825 °C over a WO_3 -promoted $\text{Ni}/\text{MgO}-\text{CaO}$ catalyst, even in the presence of H_2S [16].

Tars are relatively easy to reform, the most difficult hydrocarbon to convert being methane. Dagle et al. recently showed that the presence of benzene and naphthalene led to marked deactivations of methane conversion due to coking over Ni, Rh and Ir-based catalysts [17]. These authors had shown earlier that Rh and Ir were the most interesting metals in terms of combined activity and resistance to sintering and coking (in the absence of tars) [18]. The coking was alleviated by using higher reaction temperatures and by the presence of a noble metal. Other reports dealing with Ni-based electrodes for solid oxide fuel cells [19] and Ni and Rh-based catalysts for reforming [20] stressed that polycyclic aromatic hydrocarbons such as naphthalene and pyrene were significantly more poisonous than toluene.

Methane steam reforming is thought to be structure-sensitive with low coordination metal atoms exhibiting somewhat higher turn-over

* Corresponding author.

E-mail address: fcm@ircelyon.univ-lyon1.fr (F.C. Meunier).

frequencies (TOF) than those associated with atoms from low index planes [21–23]. A major difficulty associated with determining TOF or specific surface rates for high temperature reactions is that metal surfaces are known to be dynamic at high temperatures [24]. The formation of Ni(211) steps from Ni(111) terraces, the sites of the former surface being associated with higher TOF, was proposed to be facile due to low energy difference [25,26]. These observations stress that TOF and specific surface rates should be used with caution when based on metal surfaces or dispersions determined under conditions markedly different from those used for the catalytic test.

Ni is intrinsically less active and more difficult to disperse than noble metals [23,27], but has a significantly lower cost. Extensive carbon deposition can yet occur on Ni-based catalysts that can be of several types, i.e. pyrolytic, encapsulating and whiskers [1,25]. Encapsulating carbon (also referred to as “gum”) is typically formed during reforming of feeds containing aromatic compounds. The deposition of carbon is overall a complex interplay between methane/hydrocarbon decomposition and carbon gasification [28].

H_2S is typically present at concentration levels around 50–200 ppm in syngas derived from biomass gasification [29] and induces a marked deactivation of catalysts used for reforming [30]. The surface of Ni particles gets covered with sulfur, reaching a stoichiometry S:Ni of ca. 1:2 for surface atoms at saturation [31]. S coverage and rate loss expressions have been derived depending on the $\text{H}_2\text{S}/\text{H}_2$ ratio used [30,32]. The sulfidation of nickel surface can yet have positive effects, mainly in the suppression of carbon formation during steam reforming [33].

The effect of sulfur can be partly overcome by increasing reaction temperature, increasing H_2 pressure or modifying the electronic properties of the catalyst. Modification of the active metal to create electron-deficient sites lowers the strength of metal-sulfur bond. According to Arcoya et al. [34], the sulfur resistance of group VIII metals (investigated through arene hydrogenation) is related to the surface electronic state of the metal and increases in the following order: Pt < Pd < Ni < Rh < Ru. This order is somewhat modified when considering reaction atmospheres and temperatures similar to those typically encountered during the reforming of biomass-derived syngas (Fig. 1). Apart from iridium, Rh appears to be the most resistant to bulk sulfide formation, far more resistant than Ni. It should be stressed that the thermodynamic calculations shown in Fig. 1 regard the formation of bulk compounds and thus the stability of surface sulfide phases cannot be inferred from these calculations.

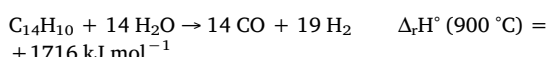
Hence Rh is expected to be more resistant to sulfur poisoning than Ni, in agreement with the data reported by Steele et al. [35], who found that Rh maintained some activity for methane steam reforming in the 800–900 °C temperature range in the presence of ca. 90 ppm of H_2S ,

while Ni-based catalysts became totally inactive. Note that a theoretical study proposed the opposite, possibly because of the choice of crystallographic planes considered [36].

Tomishige et al. [37] studied the partial oxidation of tar obtained from the gasification of a woody feedstock in a fluidized bed reactor using a 20% Ni commercial steam reforming catalyst and a 1% Rh/CeO₂/SiO₂ catalyst with and without H_2S in the feed stream. Both catalysts showed a decrease in the rate of bio-syngas formation upon the addition of H_2S , though the Rh-based catalyst deactivated markedly less than the Ni counterpart.

Lakshapatri et al. [38] assessed Ni and Rh-based catalysts for the steam reforming of heavy hydrocarbons in the presence of 1000 ppm of thiophene. While the catalysts were stable in the absence of the S-containing molecule, a marked deactivation was observed following thiophene introduction. Sulfur species were formed at the catalyst surface, but no bulk sulfides could be evidenced. These authors noted that Rh/Ni mixed metal catalysts resulted in the formation of Rh-Ni alloy species that exhibited a lower affinity towards sulfur [39]. A synergistic effect of alloying Ni with Rh in lowering S deactivation was confirmed by Xie et al. who studied the steam reforming of heavy hydrocarbons on a 10wt.%Ni-2wt.%Rh/CeO₂/SiO₂ catalyst [40].

In summary, these reports suggest that high temperatures should be preferably used to limit catalyst deactivation in the presence of tars and sulfur and that Rh-based catalysts should be more active and resistant than Ni-based samples. In the present work, a series of Rh and Ni-based catalysts were tested for the reforming of methane and phenanthrene using a feed composition similar in terms of main components to that of the gas produced from wood gasification in ECN MILENA gasifier [41]. The objective was to identify formulations that would enable reforming methane and tars without the need to purify the producer gas obtained from the gasifier. Phenanthrene was chosen as tar representative because this compound is produced in significant concentrations during low-temperature gasification of woody biomasses [42,43] and its three-ring structure favors coke formation. It should be noted that methane and especially phenanthrene reforming are highly endothermic reactions (see equations below) and thus difficulties relating to heat transport limitations can be expected.



The concentration of H_2S was set at the higher range of typical values, i.e. 200 ppm, to make these tests more challenging. The temperatures investigated were set around 900 °C to enable significant methane conversions in the presence of H_2S .

2. Experimental section

2.1. Catalyst synthesis and characterization

Eight samples containing only one metal (either Ni or Rh) or both metals were investigated (Table 1). Samples 1-Ni and 3, 4 and 5-Rh and the MgAlO_x support were supplied by Johnson Matthey and were prepared according to proprietary methods.

An ordered mesoporous crystalline magnesium-aluminum oxides support (noted “meso-MgAlO_x”) was prepared at ECN by a solvent evaporation induced self-assembling method. Pluronic P123 (Aldrich, lot MKAA0323) was dissolved in ethanol at room temperature. Nitric acid, aluminum isopropoxide, and magnesium nitrate were then added into the above solution under stirring. The mixture was covered with a polyethylene film, stirred at room temperature for about 5 h, and then put into a 100 °C drying oven to undergo solvent evaporation process. After 40 h of aging, the sample was calcined at 800 °C, leading to the sample “meso-MgAlO_x”. MgAl₂O₄ was the main phase present after calcination (not shown).

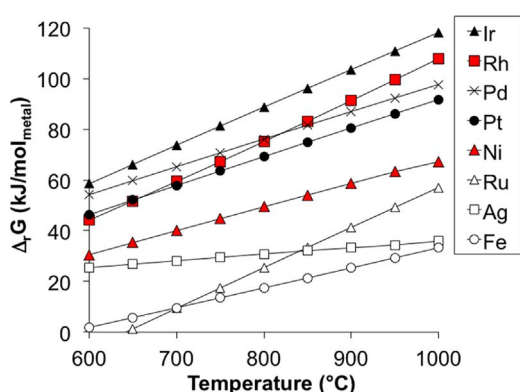


Fig. 1. Gibbs energy of reaction for the formation of metal sulfides according to the reaction $\text{M} + x \text{H}_2\text{S} \rightarrow \text{M-S}_x + x \text{H}_2$ as a function of temperature under a typical producer gas composition (i.e. 200 ppm H_2S + 20% CO + 16% H_2 + 10% CO_2 + 39% H_2O + 9% CH_4). The metal sulfides considered were IrS_x, RhS_{0.889}, PdS, PtS, NiS, RuS_x, Ag₂S and FeS. Calculated using the HSC Chemistry[®] software (Outotec, version 6).

Table 1

Composition, metal dispersion and metal surface areas of the catalysts.

Catalyst code	Support	Specific surface area ^a (m ² g ⁻¹)	Metal loading (wt.%)		Dispersion ^b (%)		Metal surface area (m ² g ⁻¹)	
			Ni	Rh	Ni	Rh	Ni	Rh
1-Ni	alumina	60	34.1	–	5.2 ± 1.8	–	11.8 ± 4	–
2-Ni	meso-MgAlOx	128 ^c	16.2	–	3.7 ± 1.3	–	4.0 ± 1.4	–
3-Rh	alumina	152	–	1.8	–	38 ± 9	–	3.0 ± 0.7
4-Rh	MgAlOx	186	–	0.4	–	43 ± 9	–	0.7 ± 0.1
5-Rh	MgAlOx	186	–	2.2	–	40 ± 10	–	3.8 ± 1.0
6-Rh	meso-MgAlOx	128 ^c	–	0.4	–	50 ± 9	–	0.8 ± 0.1
7-Rh	meso-MgAlOx	128 ^c	–	2.6	–	42 ± 7	–	4.8 ± 0.8
8-NiRh	meso-MgAlOx	128 ^c	18.6	1	4.1 ± 1.5	39 ± 7	5.1 ± 1.9 ^d	1.7 ± 0.3 ^d

^a BET method, measured on the fresh support calcined at 800 °C.^b Based on particle size measurements in TEM of used samples tested at 900 °C in absence of H₂S (200 particles were counted).^c Surface area of support before impregnation.^d Assuming that most larger particles were mostly made of Ni and most smaller particles were mostly made of Rh.

Dry impregnation was used to promote the supports with Ni and Rh. Solutions of appropriate concentrations of nickel(II) nitratehexahydrate (Aldrich lot A0348521409) and Rh(III)nitrate (Alfa Aesar, lot GR0037) were used. Bi-metallic catalysts were prepared by co-impregnation, the amount of liquid was chosen to exceed the pore volume by not more than approximately 10% which resulted in essentially incipient wetness impregnation. The metal loadings, dispersion and metal surface area are given in Table 1.

Powder X-ray diffraction patterns (XRD) were recorded to assess the crystallinity of the samples. Diffractograms were collected between 4 and 90° (2θ) with steps of 0.02° and one second per step with a Bruker D5005 diffractometer using CuKα radiation at $\lambda = 1.5418 \text{ \AA}$. Elemental analysis of the fresh catalysts was performed using an ICP-OES ACTIVA from HORIBA Jobin Yvon equipped with a CCD detector for the determination of metallic loadings. Specific surfaces of the materials (Brunauer–Emmett–Teller theory) were measured by N₂ adsorption measurements at 77 K (Belsorp-mini, BEL-Japan). Prior to measurement, raw samples were first outgassed under vacuum (< 10 Pa) at 300 °C for 4 h (Belprep, BEL-Japan).

TEM pictures were obtained using a Jeol 2010 LaB6 microscope operating at 200 kV. Particle size distributions (PSDs) were obtained by counting 200 particles using Image J software. Surface-weighted mean diameters $d_{sw} = \sum n_i d_i^2 / \sum n_i d_i^3$ were calculated from the PSDs, where n_i is the number of particles counted with a diameter d_i . Metal dispersions were deduced from the corresponding d_{sw} considering a cuboctahedral model and a calculation method described by Van Hardeveld and Hartog. Bond lengths of 2.49 and 2.69 Å; was respectively considered for Ni–Ni and Rh–Rh interactions [44]. Metal surface areas were calculated considering an atom surface area of 6.5×10^{-20} and $7.6 \times 10^{-20} \text{ m}^2$ for Ni and Rh, respectively [45]. EDX measurements were performed using an EDX Link ISIS analyzer from Oxford Instruments.

Sulfur content adsorbed at the surface of the used samples was quantified by a Flash 2000 CHONS analyzer from Thermo Scientific. A known mass of catalyst is placed in the combustion chamber under an O₂/He gas mixture flow and heated up to 1800 °C. Resulting combustion products are separated by gas chromatography where SO₂ is quantified using a thermal conductivity detector. Carbon deposits were not quantified as the corresponding CO₂ flows were below the detection limit of the TCD.

2.2. Steam reforming tests

The steam reforming experiments were performed on a lab-scale system described in details elsewhere (Fig. 2) [20]. The catalytic tests were carried out in a fixed-bed continuous-flow reactor consisting of a quartz tube (length 300 mm, 4 mm ID, 6 mm OD) containing the non-diluted catalyst held between plugs of quartz wool. The samples were

crushed and sieved into a powder retaining particle sizes between 100 and 200 µm (unless otherwise stated). Prior to testing, catalysts were reduced *in situ* at 900 °C (heating rate of 10 °C min⁻¹) for 2 h under a flow of 200 ml min⁻¹ of 20 vol.-% H₂/Ar.

A model gas composition similar to that of typical reformates was used (Table 2) [46]. Mass flow controllers (MFC) from Brooks Instrument were used to control flow rates of H₂, CH₄, CO, CO₂, N₂ and Ar. The overall system pressure was set at $P_{total} = 2.2$ bar using a needle valve located downstream the on-line analyzer. A pressure sensor was placed upstream of the reactor to check for a possible pressure increase due to bed blocking. Solid phenanthrene (C₁₄H₁₀, 3-ring polycyclic aromatic compound) was placed in a U-shaped ¼" stainless steel tube saturator in a hotbox set at 141 °C and water was placed in a 500 mL cylindrical saturator set at 99 °C. Carrier gas flow rates and saturator temperatures were chosen as to obtain the desired flow rates of steam and phenanthrene.

The catalytic bed was located in the isothermal region of a tube furnace and the temperature was monitored by a thermocouple located on the outside of the quartz tube near to the catalyst bed. 10 mg of catalyst were tested in the absence of H₂S, while 100 mg of catalyst were used in the case of H₂S-containing feeds. The bed heights varied between 0.5 and 3 mm, meaning that the reactor could not be considered in a plug-flow regime. The catalytic activity was sequentially measured according to the programs described in Fig. 3. Phenanthrene was introduced on the second leg of the programs, after 260 min.

On-line analysis of the reactor effluent was performed with a Compact GC (CGC) from Global Analyzer Solutions. The analyzer was equipped with two columns coupled with TCD and FID analyzers enabling the quantification of permanent gases (N₂, H₂, CO, CO₂ and CH₄) and hydrocarbons (CH₄ and heavier), respectively. The N₂ signal was used as an internal standard for the TCD channel to convert other peak areas into molar flows. Similarly, the CH₄ signal was used as an internal standard for the FID channel (the CH₄ molar flow rate being itself determined from the TCD channel). The quantification of water concentrations was not attempted. Quantitative analyses of permanent gases were performed by calibrating the CGC using different partial pressures of compounds diluted in N₂. On the FID channel, hydrocarbons of interest were quantified by determining their response factor relative to CH₄. Gas sampling could be carried out every 10 min.

The total gas flow rate of reactants was 125 ml min⁻¹. The corresponding WHSV was 689 h⁻¹ (respectively 69 h⁻¹) when using 10 mg (resp. 100 mg) of catalyst. Assuming catalyst density to be unity, the GHSV was 750 000 h⁻¹ (resp. 75 000 h⁻¹). These high WHSV values were used to obtain an accelerated ageing in terms of tar and sulfur exposure on a reasonable timescale. Furthermore, these conditions prevented total conversion of hydrocarbons, providing insights in terms of activity and stability of the different catalysts. Reactor modeling using the Eurokin Gas-Solid fixed bed reactor modeler [47] indicated

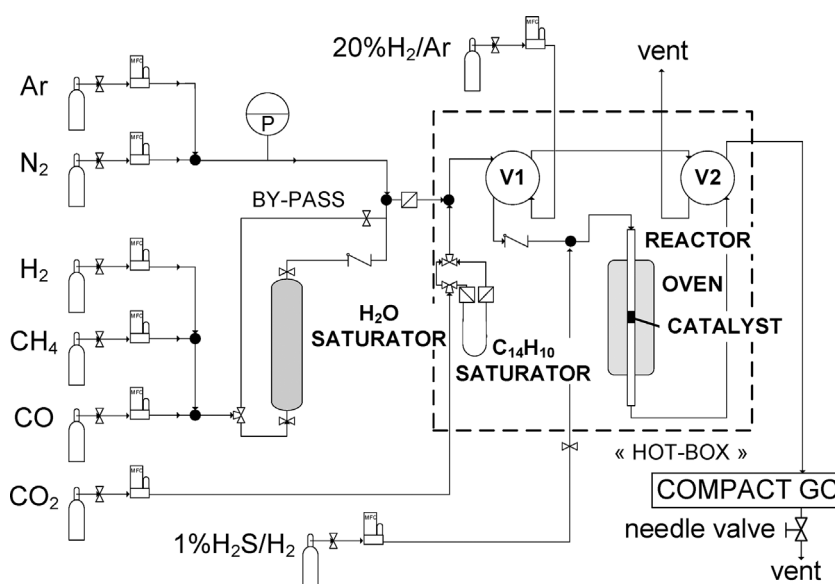


Fig. 2. Schematic layout of the experimental setup. V1 and V2 are 4-way valves.

Table 2
Feed gas composition for catalytic reforming tests (total flow rate = 125 ml min⁻¹).

Compound	CO	H ₂	CO ₂	H ₂ O	CH ₄	N ₂	Ar	Poison, if any
(vol.%)	20	16	10	39	9	2	4	Phenanthrene: 200 ppm H ₂ S: 200 ppm

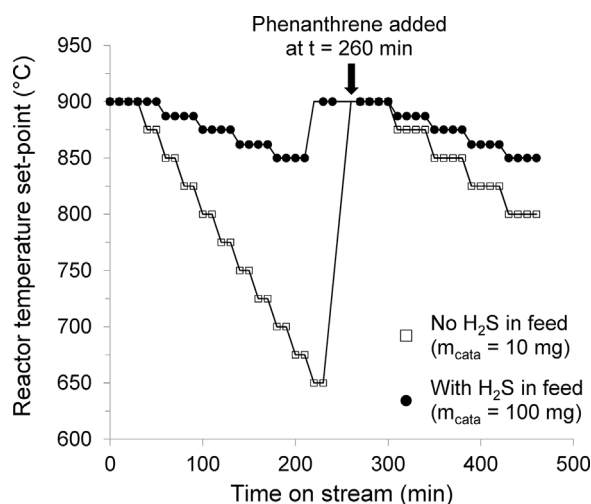


Fig. 3. Temperature profiles used for the catalytic tests with (full circles) and without (open squares) 200 ppm H₂S present in the stream. 200 ppm phenanthrene were added at 260 min. The symbols (squares and circles) represent the time at which the reactor effluent was sampled.

the presence of a significant radial heat transport limitation resulting in a cold spot of up to 45 °C when the reactor was operated at 900 °C.

3. Results and discussion

Fig. 4 gathers the logarithm of the integral rates of methane consumption measured at 900 °C over the various samples after 1h on stream. The rates measured in a feed (Table 2) free of poisons are represented by white bars. The rates appeared similar because all catalysts were highly active at this temperature and full conversion of methane was essentially achieved. The rates measured in the presence of phenanthrene (black bars) were significantly lower than those without this compound. These data thus indicate that 200 ppm of

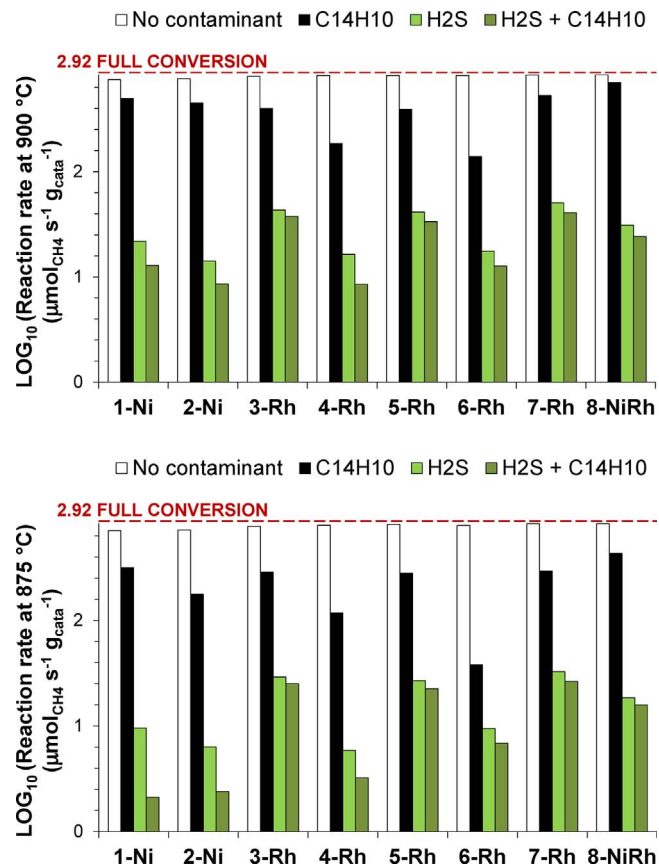


Fig. 4. Methane consumption rates measured at (Top) 900 °C and (Bottom) 875 °C over the various catalysts: (white) poison-free, (black) with 200 ppm phenanthrene, (light green) with 200 ppm H₂S and (dark green) with both 200 ppm phenanthrene and 200 ppm H₂S. (For interpretation of the references to colour in this figure legend, the reader is referred to the web version of this article.)

phenanthrene had a non-negligible poisoning effect even at 900 °C. The drop of methane consumption rate due to 200 ppm of H₂S (light green bars) was yet more than one order of magnitude larger than that associated with phenanthrene (black bars). The conversion of methane in the presence of H₂S was typically always lower than 60%. The activity loss obtained when both poisons were present (dark green bars)

was marginally lower than those obtained with H_2S only (light green bars).

A similar set of data collected at 875 °C is also shown in Fig. 4. The detrimental effects of phenanthrene (black bars) was more obvious than that observed at 900 °C, though the drop of the true intrinsic rate cannot be exactly determined because methane conversions were too high. The rate decays induced by H_2S were here again more than one order of magnitude larger than those associated with phenanthrene. The combined effect of both poisons was similar to that of only H_2S , although the two formulations based only on Ni showed a significantly worse loss.

Both sets of data at 900 °C and 875 °C clearly indicate that H_2S was the most potent poison in the present conditions and that the further effect of phenanthrene was minor, except for formulation purely based on Ni (i.e. 1-Ni and 2-Ni). The three most active formulations in the presence of both poisons all contained Rh (i.e. 3-Rh, 5-Rh and 7-Rh). While Ni only-based formulation were significantly less active, it should nonetheless be stressed that non-zero rates were measured.

The effect of lowering the temperature down to 850 °C on the value of the integral methane consumption rate when both poisons were present is compared to the cases at 900 and 875 °C in Fig. 5. Most importantly, samples purely based on Ni (i.e. 1-Ni and 2-Ni) became essentially inactive at 850 °C. In contrast, the Rh-based samples still exhibited a significant rate, especially the three best formulations highlighted above.

The integral rates of methane reforming in the presence of H_2S and phenanthrene are plotted as a function of the Ni or Rh metal surface areas in Fig. 6. The metal dispersions were measured on the samples used up to 900 °C in the standard feed in the presence phenanthrene, but in the absence of H_2S . Hepola et al. have suggested that the surface of sulfided Ni could reconstruct under high pressure of H_2S [48]. Yet, H_2S is not expected to modify metal particle size, merely leading to sulfur adlayers with $\text{S:Ni} = 0.5$ in the case of nickel-based catalysts [30,31]. No such observations have yet been reported for Rh-based catalysts. Sample 8-NiRh contained both Ni and Rh and is reported twice in the figure, with respect to the corresponding Ni and Rh areas, assuming that the smaller (respectively larger) particles observed by TEM were predominantly made of Rh (resp. Ni).

The rate values measured for metal surface areas of ca. $4 \text{ m}^2 \text{ g}^{-1}$ for the 2-Ni and Rh-based samples (i.e. 3-, 5- and 7-Rh) indicated that Rh was about five-fold more active than Ni (Fig. 6). Note that the rate of 1-Ni was not used for the comparison, because it was likely disguised by heat transfer limitations at this temperature (*vide infra*). The higher activity of Rh as compared to Ni in the presence of H_2S has been reported by Steele et al. [35]. Note that this is in contrast with the data reported in S-free feeds for which Ni appears to be intrinsically more

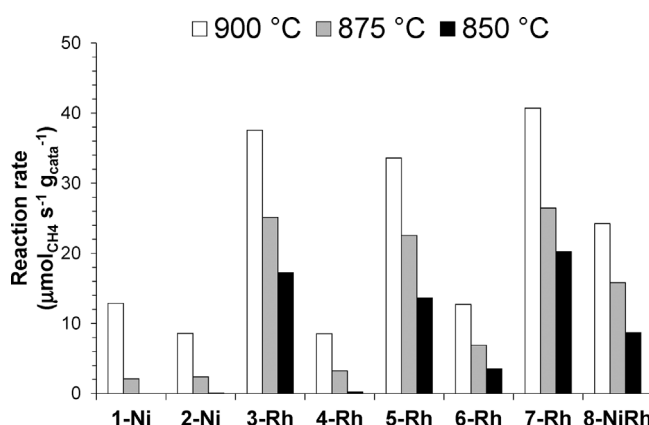


Fig. 5. Methane consumption rates measured at 900, 875 and 850 °C over the various catalysts with both 200 ppm of phenanthrene and 200 ppm of H_2S . Full methane conversion corresponds to an integral rate of $84 \mu\text{mol}_{\text{CH}_4} \text{ s}^{-1} \text{ g}_{\text{cata}}^{-1}$.

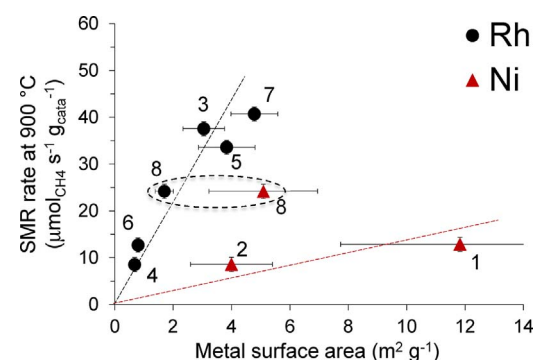


Fig. 6. Methane consumption rates measured at 900 °C in the presence of H_2S and phenanthrene over the various catalysts as a function of Ni or Rh metal surface area. The number X beside the data points refers to X-Ni or X-Rh. The triangles refer to Ni, while the circles refer to Rh. Sample 8-NiRh contained both Ni and Rh and is therefore reported twice, with respect to the corresponding Ni and Rh areas, assuming that the smaller (respectively larger) particles observed by TEM were predominantly made of Rh (resp. Ni).

active than Rh [23].

The methane consumption rates for Rh-containing samples (circles) appeared to be essentially proportional to the Rh metal surface area (Fig. 6). This indicates that methane consumption rate was associated with Rh surface atoms under the present conditions for these samples.

The data regarding methane consumption rates for Ni-containing samples (triangles) are more difficult to interpret because of the fewer samples investigated and the fact that one of those also contained Rh (i.e. 8-NiRh). Since Rh is significantly more active than Ni in the presence of H_2S , samples 8-NiRh cannot be used to evaluate any activity trend with respect to Ni content. Therefore, only samples 1-Ni and 2-Ni can be discussed. The rate measured over sample 1-Ni appeared lower than expected if a linear relationship (including the origin) was sought. This could be related to heat transport limitations in the case of this highly Ni loaded (34 wt.%), as described later (*vide infra*).

The sulfur-content of the Rh-only-based catalysts were measured post-reaction. It appears that the uptake of sulfur was essentially proportional to the surface area of Rh, with a S:Rh molar ratio of about 0.5 (Fig. 7). It is interesting to note that surface saturation with sulfur occurs at the same ratio for Ni-based catalysts [28,32]. This observation is consistent with an earlier report on the adsorption of H_2S onto Rh(100) surface, which pointed to a S:Rh ratio of ca. 0.53 at saturation [49]. It should be stressed that active sites for methane reforming are thought to be step sites, hence representing only a fraction of total surface sites [25]. Therefore, the global surface sulfidation ratio may not be representative of that of active sites.

Phenanthrene conversions were total for all samples at 850, 875 and 900 °C in the absence of H_2S and neither benzene nor naphthalene

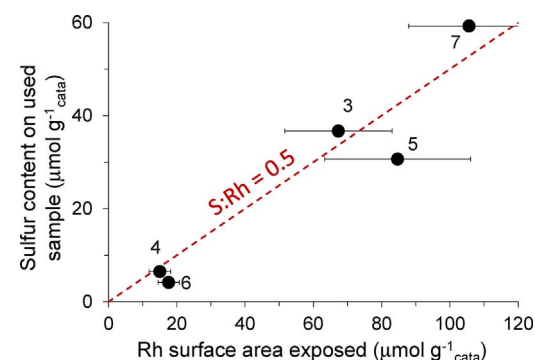


Fig. 7. Sulfur content present on used samples as a function of the exposed Rh surface area for the various monometallic catalysts. The observed S:Rh molar ratio is close to 0.5. The number X beside the data points refers to X-Rh.

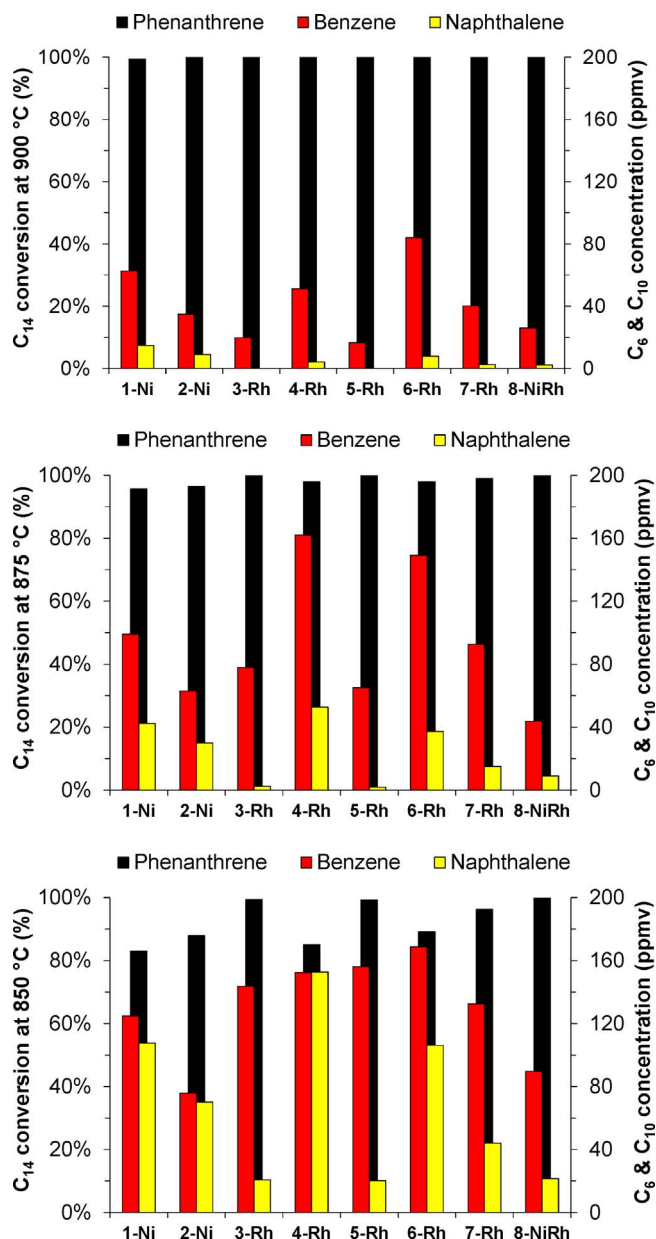


Fig. 8. Phenanthrene conversion (C₁₄, black), benzene (C₆, red) and naphthalene (C₁₀, yellow) concentrations at 900 °C (top), 875 °C (middle) and 850 °C (bottom) over the various catalysts in the presence of both 200 ppm phenanthrene and 200 ppm H₂S. Catalyst mass = 100 mg. (For interpretation of the references to colour in this figure legend, the reader is referred to the web version of this article.)

could be detected at the reactor exhaust (data not shown). Essentially total conversion of phenanthrene was also obtained in the presence of H₂S at 900 and 875 °C, though in this case significant concentrations of benzene and naphthalene were observed at the reactor exit (Fig. 8). In contrast, the reaction carried out at 850 °C led to incomplete phenanthrene conversion for several formulations and also led to increased concentrations of naphthalene. The catalysts were therefore less able to reform polycyclic aromatic hydrocarbons at 875 °C and especially at 850 °C. This is a major shortcoming, since polycyclic aromatic hydrocarbons are most detrimental in terms of coke formation [25]. Therefore, long-term process durability could be jeopardized if too low reaction temperatures are used, even on the best Rh-based samples.

The use of mesoporous supports has been reported to favour the stabilisation of metal nano-particles during catalytic reactions [50]. Table 3 shows the relative loss in metal surface area during (H₂S-free

Table 3
Evolution of dispersion and metal surface area during H₂S-free reforming.

Catalyst	Metal dispersion (%)		Metal surface area (m ² g ⁻¹)		Loss in metal surface area after use (%)
	Activated	Used	Activated	Used	
1-Ni	9.4	5.9	21.4	13.4	37
2-Ni (meso)	7.4	3.7	8.0	4.0	50
3-Rh	59.5	38.5	4.7	3.0	35
6-Rh (meso)	69.3	50.4	1.0	0.8	20
7-Rh (meso)	55.0	41.8	5.9	4.8	19

reforming for some Ni and Rh-based samples. No beneficial effect of the mesoporous support was observed in the case of Ni, since the sample based on a mesoporous support (2-Ni) had lost more metal surface area after use than a non-mesoporous sample (1-Ni) had. In contrast, the rhodium catalysts based on a mesoporous support (6-Rh and 7-Rh) exhibited a more limited loss of metal surface area upon use than one based on a non-mesoporous support (3-Rh). Differences in intrinsic properties such as Tamman temperature of Ni (MP = 1455 °C) and Rh (MP = 1964 °C) or the initial metal particle size could explain these behaviors, but more work would clearly be needed to rationalize these observations.

The apparent activation energies (E_{app}) measured for methane consumption for the various samples in the absence of poisons (white bars) appeared to vary from 56 to 104 kJ mol⁻¹ (Fig. 9). The E_{app} was determined from the activity for methane reforming measured between 650–750 °C. The methane conversion was typically below 50%, though differential conditions were not achieved. These values should therefore be taken as gross estimates. The E_{app} values reported by Wei and Iglesia [27] for methane steam reforming are ca. 102 and 109 kJ mol⁻¹ for Ni and Rh-based catalysts, respectively (represented by red lines in Fig. 9). It is worth noting that the 1-Ni catalyst exhibited an E_{app} of 101 ± 4 kJ mol⁻¹, this is identical to the value obtained by Wei and Iglesia [27] under gradientless conditions, thus supporting the absence of mass transport limitations for the 1-Ni sample at these low temperatures.

The occurrence of internal mass transport limitation was checked for the mesopore-based sample 2-Ni that led to the lowest E_{app}. Two different particle size fractions were used and the sample with the smallest particle sizes (< 100 µm) led to an Arrhenius plot essentially parallel to that of the 1-Ni sample (Fig. 10) with an E_{app} of 96 ± 9 kJ mol⁻¹, supporting the absence of mass transport limitations for in this case. In contrast, the slope of the Arrhenius plot

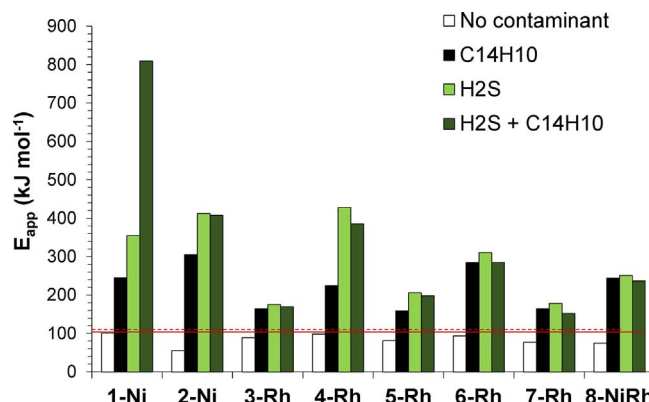


Fig. 9. Apparent activation energies for methane consumption for the various samples under various feeds: (white) poison-free, (black) with 200 ppm phenanthrene, (light green) with 200 ppm H₂S and (dark green) with both 200 ppm phenanthrene and 200 ppm H₂S. E_{app} values measured by Wei and Iglesia [27] in SMR on Ni (red full line) and Rh (red dashed line) are also reported. (For interpretation of the references to colour in this figure legend, the reader is referred to the web version of this article.)

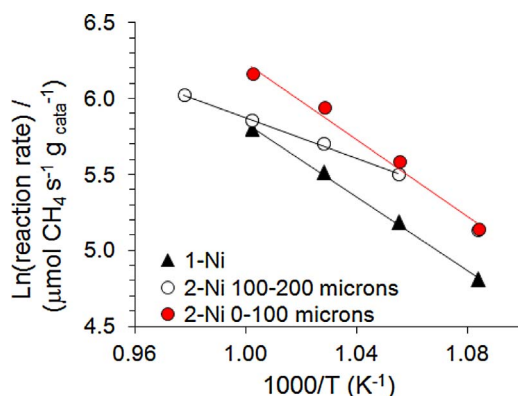


Fig. 10. Arrhenius-type plots for 1-Ni and 2-Ni samples showing the logarithm of the methane consumption rate versus the reciprocal temperature (temperature range: 650–750 °C) under a poison-free feed. Two different size distributions are compared for the 2-Ni sample.

corresponding to the 2-Ni sample with the usual larger size fraction (between 100 and 200 μm) was significantly lower (Fig. 10), yielded an E_{app} 56 ± 5 kJ mol⁻¹. These results supports the occurrence of internal mass transport limitations in the case of this particular sample and possibly in the case of the other samples based on the same support. This mass transport limitation would likely be exacerbated at higher temperatures. Reactor modeling using the Eurokin Gas-Solid fixed bed reactor modeler [47] supported this analysis (data not shown). The distribution of metal nanoparticles within the support pore system was not checked (e.g. by TEM tomography), as this could affect the mass transfer limitation depending on the distribution, e.g. metal nanoparticles near the pore mouth or deeply buried in the particle core.

Similar reactor modeling indicated the presence of a significant radial heat transport limitation resulting in a cold spot of up to 45 °C when the reactor was operated at 900 °C without diluent (data not shown).

An additional experiment was carried out diluting the catalyst in an inert material to facilitate heat exchange with the reactor walls (Fig. 11). The observed reaction rate was significantly higher, confirming the occurrence of heat transport limitations. Therefore it is clear that the present activity measurements were disguised with heat and mass transport limitations. This observation probably explains why the rate data reported in Fig. 6 actually displayed a curve with a somewhat decreasing slope at higher metal surface areas, rather than a perfect straight line.

The TOF obtained under our conditions were compared to those reported by Wei and Iglesia [27], which were obtained in the absence of

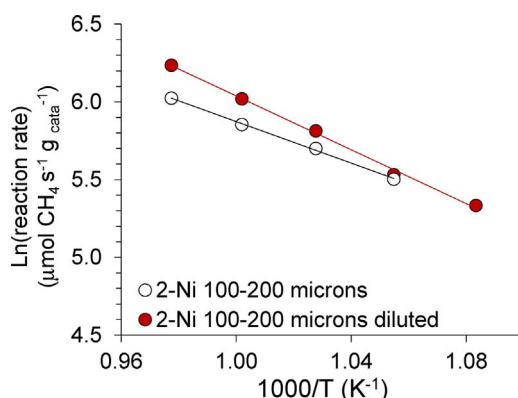


Fig. 11. Arrhenius-type plots for 2-Ni sample showing the logarithm of the methane consumption rate versus the reciprocal temperature (temperature range: 650–750 °C) under a poison-free feed. One experiment was realized diluting 10 mg of 2-Ni with 28 mg of α-Al₂O₃, another one was carried out without dilution.

mass and heat transport limitations (Fig. 12). The data of these authors obtained at 600 °C were extrapolated to 650 °C using an E_{app} of 109 kJ/mol. Differences in reactant concentrations were corrected assuming a reaction first order with respect to CH₄ and zeroth-order with respect to water. The TOF plotted as a function of Rh dispersion (Fig. 12, right) were clearly lower than those measured by Wei and Iglesia [27], stressing the non-intrinsic nature of the TOF measured under our conditions.

The apparent activation energies measured in the presence of phenanthrene and H₂S were markedly higher than those observed without these poisons (Fig. 9). Two and even eight-fold increases were noted. Most E_{app} values were comprised between 150 and 400 kJ/mol in the presence of both pollutants, but a value as high as 800 kJ/mol was calculated for 1-Ni. E_{app} values in the range 260–290 kJ/mol had been reported [30] in the case of Ni-based samples used in the presence of up to 300 ppm of H₂S, consistent with the data reported here. These exceedingly high values were most likely due a variation of the number of metal sites active for CH₄ reforming with temperature as a result of changes of the surface coverage of sulfur and carbonaceous deposits. It should be yet noted that our best three formulations (i.e. 3-Rh, 5-Rh and 7-Rh) exhibited E_{app} the closest to the values reported by Wei and Iglesia [27].

The observed E_{app} values will therefore encompass terms for the heat of adsorption of both sulfur and carbonaceous surface species, in addition to those due to the adsorption of the reactants, i.e., methane, water and CO₂ [51,52]. Alstrup et al. [32] have reported a heat of adsorption of ca. 289 kJ/mol for H₂S on Ni-based catalyst and the heat of sublimation of phenanthrene is ca. 91 kJ/mol. It is therefore impossible to extract any direct kinetic (e.g. TOF) or thermodynamic (heat of adsorption) information from these temperature-dependent data apart from specific reaction rates, due to the complexity of the system (i.e. high number of reactants and many by-products).

The slope of the curve representing the methane consumption rate as a function of the Rh metal surface area appeared to somewhat decrease at higher values (Fig. 6). This was likely associated with local temperature decrease on the more active samples due to the endothermic nature of the reforming reactions and heat transport limitations, as suggested by the dilution experiments realized on 2-Ni (Fig. 11). These observations raise the question as to what would be a suitable active site concentration in the reactor, for a fixed quantity of active sites and reactor diameter. An infinite dilution of sites would alleviate cold spot effects, but of course requires a longer reactor. Highly concentrated sites, typically achieved by increasing metal loading, would enable using very short reactors but cold spots would decrease catalyst activity.

A reactor model developed for the autothermal reforming of methane [53] was adapted to represent the present reforming conditions and reactor diameter and used to determine the evolution of methane conversion with bed length. Methane conversion (i.e. 54%) measured over a 2 cm-bed length of sample 3-Rh at 900 °C was used as reference point (Fig. 13).

The corresponded calculated temperature drop (cold spot) was ca. 40 °C, similar to that predicted by the Eurokin modeler (*vide supra*). Our model suggest that very little conversion gain would be achieved by decreasing site density using longer bed length (Fig. 13), stressing that in the present case catalyst effectiveness factor was close to 1. This stresses that most of our data were only slightly affected by the non-isothermal nature of the reactor.

In contrast, a conversion drop of from 53% down to 38% would be obtained by increasing eight-fold the density of active site (bed length decreased from 2 cm down to 0.25 cm). The corresponding cold spot would be as high as 120 °C. These calculations indicate that it would be counterproductive to concentrate too many active sites and that the concentration used in the present work (reference point in Fig. 13) offers an acceptable compromise between short bed length and sample activity.

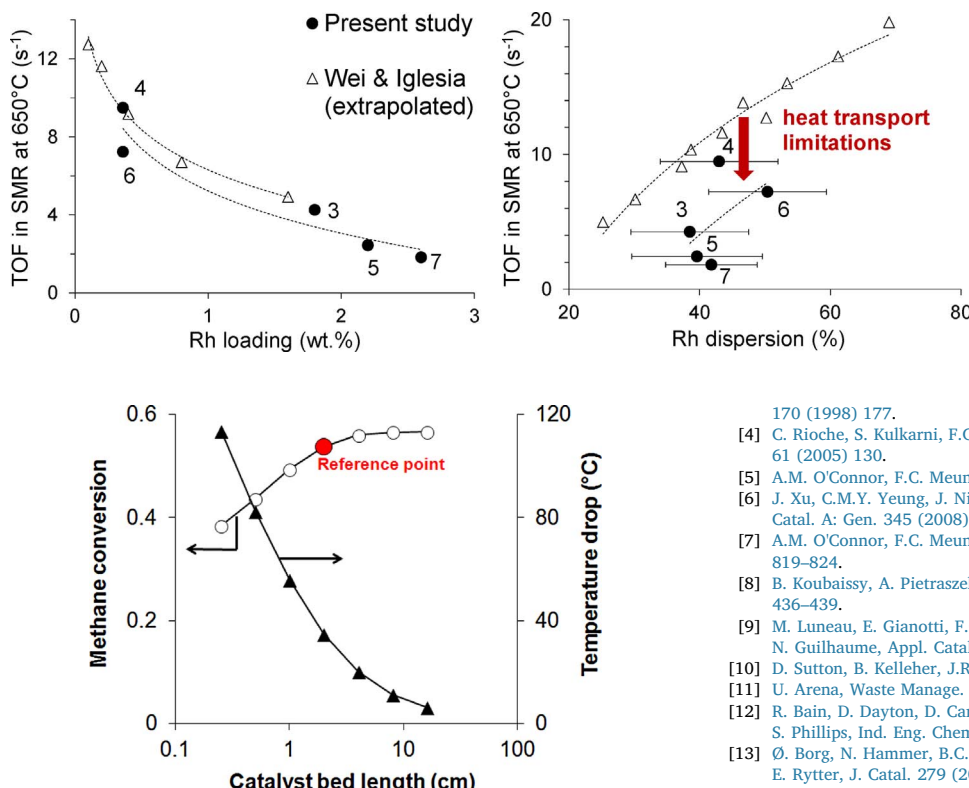


Fig. 13. Modeling of methane conversion (circles) and highest temperature drop in the catalyst bed (triangles) as a function of the catalyst bed length. The number of active sites was kept constant. The thermal conductivity of alumina was used for heat transport calculations. Reactor internal diameter = 4 mm, oven (=inlet) temperature = 900 °C.

Activity tests carried out on much longer time-scale (several days) at high temperatures (ca. 900 °C) in the presence of both phenanthrene and H₂S will be necessary to ascertain the commercial potential of the best formulations investigated here and are in progress.

4. Conclusions

200 ppm of H₂S led to a significantly higher loss of activity during the reforming of methane than that induced by 200 ppm of phenanthrene over a series of Ni and Rh-based catalysts used at 900 °C. The rate of methane conversion in the presence of both poisons varied linearly with Rh metal surface area. The slight deviation observed at higher loadings was in part due to heat and mass transport limitations. The rate of methane consumption per unit of metal surface area was ca. 5-fold higher on Rh as compared to the case of Ni. No information could be derived from the measure of apparent activation energies, due to changes in adsorption coverage of reactants and poisons with temperature. The use of lower temperatures (875 °C and especially 850 °C) led to incomplete conversion of polyaromatics, which are well-known coke precursors.

Acknowledgment

This work was partly supported by the European Union Seventh Framework Programme FP7-NMP-2013, under Grant Agreement number 604277 (acronym FASTCARD).

References

- [1] J.R. Rostrup-Nielsen, J. Sehested, J.K. Norskov, *Adv. Catal.* 47 (2002) 65.
- [2] G. Jones, J. Jakobsen, S. Shim, J. Kleis, M. Andersson, J. Rossmeis, F. Abildpedersen, T. Bligaard, S. Helveg, B. Hinnemann, *J. Catal.* 259 (2008) 147.
- [3] P. Ferreira-Aparicio, A. Guerrero-Ruiz, I. Rodriguez-Ramos, *Appl. Catal. A: Gen.* 360 (2009) 170 (1998) 177.
- [4] C. Rioche, S. Kulkarni, F.C. Meunier, J.P. Breen, R. Burch, *Appl. Catal. B: Environ.* 61 (2005) 130.
- [5] A.M. O'Connor, F.C. Meunier, J.R.H. Ross, *Stud. Surf. Sci. Catal.* 119 (1998) 819.
- [6] J. Xu, C.M.Y. Yeung, J. Ni, F. Meunier, N. Acerbi, M. Fowles, S.C. Tsang, *Appl. Catal. A: Gen.* 345 (2008) 119.
- [7] A.M. O'Connor, F.C. Meunier, J.R.H. Ross, *Stud. Surf. Sci. Catal.* 119 (1998) 819–824.
- [8] B. Koubaisy, A. Pietraszek, A.C. Roger, A. Kienemann, *Catal. Today* 157 (2010) 436–439.
- [9] M. Luneau, E. Gianotti, F.C. Meunier, C. Mirodatos, E. Puzenat, Y. Schuurman, N. Guilhaume, *Appl. Catal. B: Environ.* 203 (2017) 289.
- [10] D. Sutton, B. Kelleher, J.R.H. Ross, *Fuel Proc. Technol.* 73 (2001) 155.
- [11] U. Arena, *Waste Manage.* 32 (2012) 625.
- [12] R. Bain, D. Dayton, D. Carpenter, S. Czernik, C. Feik, R. French, K. Magrini-Bair, S. Phillips, *Ind. Eng. Chem. Res.* 44 (2005) 7945.
- [13] Ø. Borg, N. Hammer, B.C. Enger, R. Myrstad, O.A. Lindvåg, S. Eri, T.H. Skagseth, E. Ryter, *J. Catal.* 279 (2011) 163.
- [14] S. Chitsazan, S. Sepehri, G. Garbarino, M.M. Carnasciali, G. Busca, *Appl. Catal. B: Environ.* 187 (2016) 386–398.
- [15] A. Di Carlo, D. Borello, M. Sisinni, E. Savuto, P. Venturini, E. Bocci, K. Kuramoto, *Int. J. Hydrogen Energy* 40 (2015) 9088.
- [16] K. Sato, K. Fujimoto, *Catal. Commun.* 8 (2007) 1697.
- [17] V.L. Dagle, R. Dagle, L. Kovarik, A. Genc, Y.-G. Wang, M. Bowden, H. Wan, M. Flake, V.-A. Glezakou, D.L. King, R. Rousseau, *Appl. Catal. B: Environ.* 184 (2016) 142.
- [18] D. Mei, V.-A. Glezakou, V. Lebarbier, L. Kovarik, H. Wan, K.O. Albrecht, M. Gerber, R. Rousseau, R.A. Dagle, *J. Catal.* 316 (2014) 11–23.
- [19] N. Dekker, J.P. Ouweltjes, S. Linnekamp, B. Rietveld, *ECS Trans.* 7 (2007) 1465–1473.
- [20] D. Laprune, C. Theodoridi, A. Tuel, D. Farrusseng, F.C. Meunier, *Appl. Catal. B: Environ.* 204 (2017) 515.
- [21] H.S. Bengaard, J.K. Norskov, J. Sehested, B.S. Clausen, L.P. Nielsen, A.M. Molenbroek, J.R. Rostrup-Nielsen, *J. Catal.* 209 (2002) 365.
- [22] Y. Wang, Y.H. Chin, R.T. Rozmiarek, B.R. Johnson, Y. Gao, J. Watson, A.Y.L. Tonkovich, D.P. Vander Wiel, *Catal. Today* 98 (2004) 575.
- [23] A. Yamaguchi, E. Iglesia, *J. Catal.* 274 (2010) 52.
- [24] S. Helveg, C. Lopez-Cartes, J. Sehested, P.L. Hansen, B.S. Clausen, J.R. Rostrup-Nielsen, F. Abild-Pedersen, J.K. Norskov, *Nature* 427 (2004) 426.
- [25] J. Sehested, *Catal. Today* 111 (2006) 103.
- [26] H.S. Bengaard, Ph.D. Thesis, Danish Technical University, 2001.
- [27] J. Wei, E. Iglesia, *J. Catal.* 224 (2004) 370.
- [28] C.A. Bernardo, I. Alstrup, J.R. Rostrup-Nielsen, *J. Catal.* 96 (1985) 517.
- [29] P. Simell, E. Kurkela, P. Ståhlberg, J. Hepola, *Catal. Today* 27 (1996) 55.
- [30] J. Koning, K. Sjostrom, *Ind. Eng. Chem. Res.* 37 (1998) 341.
- [31] M. Perdereau, J. Oudar, *Surf. Sci.* 20 (1970) 80.
- [32] I. Alstrup, J.R. Rostrup-Nielsen, S. Roen, *Appl. Catal. A* 1 (1981) 303.
- [33] J.R. Rostrup-Nielsen, *J. Catal.* 85 (1984) 31.
- [34] A. Arcoya, A. Cortes, J. Fierro, X. Seoane, *Stud. Surf. Sci. Catal.* 68 (1991) 557.
- [35] A.M. Steele, S. Pouston, K. Magrini-Bair, W. Jablonski, *Catal. Today* 214 (2013) 74.
- [36] K. Lee, C. Song, M. Janik, *Langmuir* 28 (2012) 5660.
- [37] K. Tomishige, T. Miyazawa, T. Kimura, K. Kunimori, N. Koizumi, M. Yamada, *Appl. Catal. B: Environ.* 60 (2005) 299.
- [38] S. Lakhpatri, M. Abraham, *Appl. Catal. A: Gen.* 364 (2009) 113.
- [39] S. Lakhpatri, M. Abraham, *Catal. Sci. Technol.* 3 (2013) 2755.
- [40] C. Xie, Y. Chen, Y. Li, X. Wang, C. Song, *Appl. Catal. A: Gen.* 390 (2010) 210.
- [41] C.M. van der Meijden, A. van der Drift, B.J. Vreugdenhil, 15th European Biomass Conference, 7–11 May 2007, Berlin, Germany, 2017 ECN report ECN-M-08-083 available at <http://www.ecn.nl/docs/library/report/2008/m08083.pdf>.
- [42] U. Wolfsberger, I. Aigner, H. Hofbauer, *Environ. Prog. Sustainable Energy* 28 (2009) 372.
- [43] <https://www.ecn.nl/docs/library/report/2010/e10008.pdf>.
- [44] L. Sutton, Table of interatomic distances and configuration in molecules and ions (supplement 1956–1959), *Lond. Chem. Soc.* 18 (1965).
- [45] H. Liu, *Ammonia Synthesis Catalysts: Innovation and Practice*, (2013), p. 586 978-981-4355-77-3.
- [46] M. van der Meijden, P.C.A. Bergman, A. van der Drift, B.J. Vreugdenhil, Preparations for a 10 MWth Bio-CHP, 18th European Biomass Conference and

Exhibition, 3–7 May 2010, Lyon, France, 2017.

[47] <http://eurokin.tudelft.nl/>.

[48] J. Hepola, J. McCarty, G. Krishnan, V. Wong, *Appl. Catal. B: Environ.* 20 (1999) 191–203.

[49] R.I. Hegde, J.M. White, *J. Phys. Chem.* 90 (1986) 296.

[50] K.-J. Chao, M.-H. Cheng, Y.-F. Ho, *Catal. Today* 97 (2004) 49–53.

[51] M. Temkin, *Acta Physicochim. URSS* 3 (1935) 312.

[52] G.C. Bond, *Catal. Today* 49 (1999) 41–48.

[53] M. Luneau, Elia Gianotti, N. Guilhaume, E. Landrivon, F.C. Meunier, C. Mirodatos, Y. Schuurman, *Ind. Eng. Chem. Res.*, in press 10.1021/acs.iecr.7b01559.